Effect of $3d$ ion substitution in the $R\mathrm{Ba_2Cu_{3-x}}M_x\mathrm{O_7}$ (R=Sm, Dy; M=Fe, Ni and Zn) system: Implications of R ion dependence and disorder

P. Sumana Prabhu and U. V. Varadaraju
Materials Science Research Centre, Indian Institute of Technology, Madras 600 036, India
(Received 2 October 1995)

Systematic studies on the $R\mathrm{Ba_2Cu_{3-x}}M_x\mathrm{O_7}$ (R=Sm, Dy; M=Fe, Ni, Zn) system were carried out in order to determine the effect of the rare-earth ionic size and magnetic moment on the T_c suppression rate. The phases were characterized by powder x-ray diffraction (XRD), resistivity, and ac susceptibility measurements. XRD studies indicate a higher solubility limit of M ions in the $\mathrm{SmBa_2Cu_{3-x}}M_x\mathrm{O_7}$ [Sm-123(M)] system as compared to the $\mathrm{DyBa_2Cu_{3-x}}M_x\mathrm{O_7}$ [Dy-123(M)] system. Resistivity and ac susceptibility studies indicate that the T_c suppression rate for a given M ion depends on the ionic radius of the rare earth (R) and is higher for larger rare earths. The trend in T_c suppression as a function of concentration (x) shows deviation from Abrikosov-Gor'kov behavior. A metal-insulator transition is observed at higher dopant concentrations, and the semiconducting phases are found to obey the Mott's variable range hopping mechanism of conduction. The parameters related to hopping conduction; viz., the characteristic temperature (T_0), localization length (a), hopping range (R), and hop energy (W) have been calculated, and a comparative study of the variation of these parameters in the two systems has been made. [S0163-1829(96)02518-0]

I. INTRODUCTION

Among the high-T_c oxide superconductors, the $\mathrm{YBa_2Cu_3O_{7-\delta}}$ system has been well studied with regard to structural as well as the physical properties. In the pure $R\mathrm{Ba_2Cu_3O_7}$ (R=rare earth) system, T_c remains unchanged for all R ions irrespective of their magnetic moments[1,2] except for R=Pr. However, substitution at the Cu site by $3d$ metal ions has a dramatic effect on T_c, since the $\mathrm{CuO_2}$ planes are responsible for superconductivity and any substitution at this site depresses T_c, independent of whether the substituent ion is magnetic or nonmagnetic. Substitutional studies in the $\mathrm{NdBa_2Cu_{3-x}}M_x\mathrm{O_7}$ (M=Fe, Ni, Zn) system have shown an increase in the solid solubility limits (x) as well as the T_c, suppression rates.[3] A similar R ion dependence has been observed in other systems.[4–6] This has been attributed to the decrease in the spatial extension of the $4f$ orbitals of the R ion with decrease in the ionic radius.[5] It appears, therefore, that simultaneous substitution of a rare-earth ion at the Y site and $3d$ metal ion at the Cu site modifies the nature of interaction of the $4f$ orbitals of the R ion with the $\mathrm{CuO_2}$ planes. In the present study, we have carried out systematic substitutional studies on $R\mathrm{Ba_2Cu_{3-x}}M_x\mathrm{O_7}$ (R=Sm, Dy; M=Fe, Ni, Zn) with the following objectives: (i) to determine the effect of the magnetic moment and the ionic radius of the rare-earth ion on the T_c suppression rates and (ii) to make a comparative study of the parameters related to the variable-range-hopping mechanism of conduction in the semiconducting phases of the two systems, viz., the characteristic temperature (T_0), localization length (a), hopping length (R), and hop energy (W).

II. EXPERIMENTAL DETAILS

A total of about 70 compositions of $R\mathrm{Ba_2Cu_{3-x}}M_x\mathrm{O_7}$ (R=Sm, Dy; M=Fe, Ni, Zn: $0.0 \leqslant x \leqslant 0.1$ in steps of 0.02 and $0.1 \leqslant x \leqslant 0.8$ in steps of 0.1) were synthesised using the conventional solid-state reaction method. The starting materials $R_2\mathrm{O_3}$ (R=Sm, Dy; 99.99% IRE), $\mathrm{BaCO_3}$ (99.99%, Cerac), CuO (99.999%, Cerac), and $\mathrm{Fe_2O_3}$/NiO/ZnO (99.9%, Cerac) were taken in stoichiometric proportions, ground thoroughly, and heated at 920 °C for 24 h followed by 940 °C for 24 h with intermediate grinding. The powder was pressed into pellets (diameters 8 and 12 mm, thicknesses 1–2 mm; WC-lined stainless-steel die; 4–5 tons/cm^2 pressure) and sintered at 940 °C for 24 h followed by furnace cooling to room temperature (RT). Oxygen treatment was carried out at 900 °C for 24 h followed by 600 °C for 24 h and furnace cooled to RT. The phases were characterized by powder x-ray diffraction (XRD) using Cu $K\alpha$ radiation (Seifert, Germany, model P3000). Resistivity measurements were carried out by the four-probe Van der Pauw method using a closed-cycle He refrigerator (Leybold Hareaus). ac susceptibility measurements in the range 300–13 K were made with a field of 0.1 Oe and frequency 300 Hz using an automated Sumitomo Superconducting Materials Property Measuring Equipment (model SCR 204-T, Japan).

III. RESULTS

A. Structure and stoichiometry

1. $SmBa_2Cu_{3-x}M_xO_7$ system (M=Fe, Ni, Zn)

All compositions of the system $\mathrm{SmBa_2Cu_{3-x}}M_x\mathrm{O_7}$ (M=Fe, Ni, Zn) are black in color and stable under normal atmospheric conditions. XRD studies indicate well-defined sharp peaks, and for lower values of x, highly oriented ($00l$) lines are obtained. The upper limit of solid solubility is x=0.8 for all M. This is much higher than that reported for the $\mathrm{YBa_2Cu_{3-x}}M_x\mathrm{O_7}$ system where the maximum solid solubility limits of $3d$ metal ions are x=0.6 for M=Fe and 0.3 for M=Ni, Zn. In the $\mathrm{NdBa_2Cu_{3-x}Fe_xO_7}$ system, the solid solubility limit of Fe is about 1.0.[3] Slater *et al.*[7] have reported the maximum solid solubility of Fe in

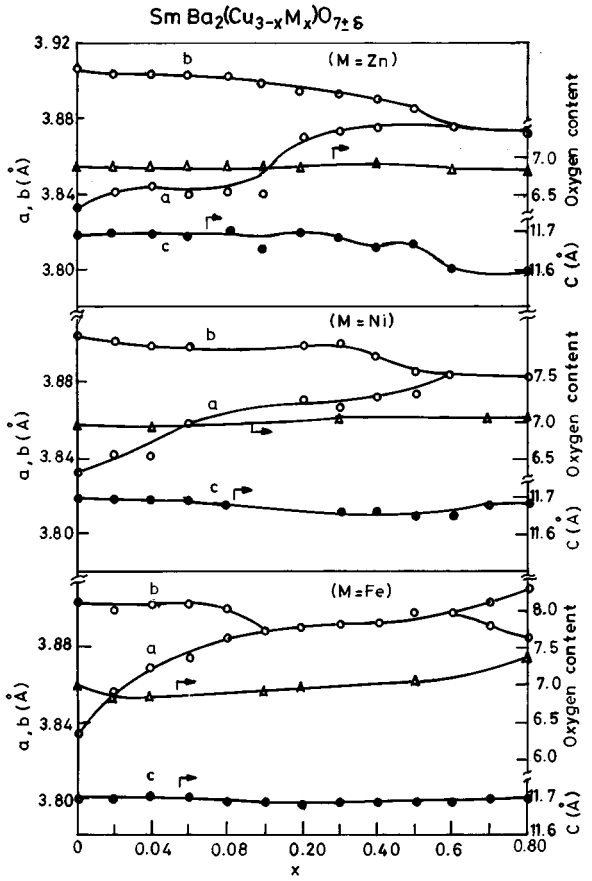

FIG. 1. Variation of lattice parameters and oxygen content as a function of concentration (x) in the $SmBa_2(Cu_{3-x}M_x)O_7$ system.

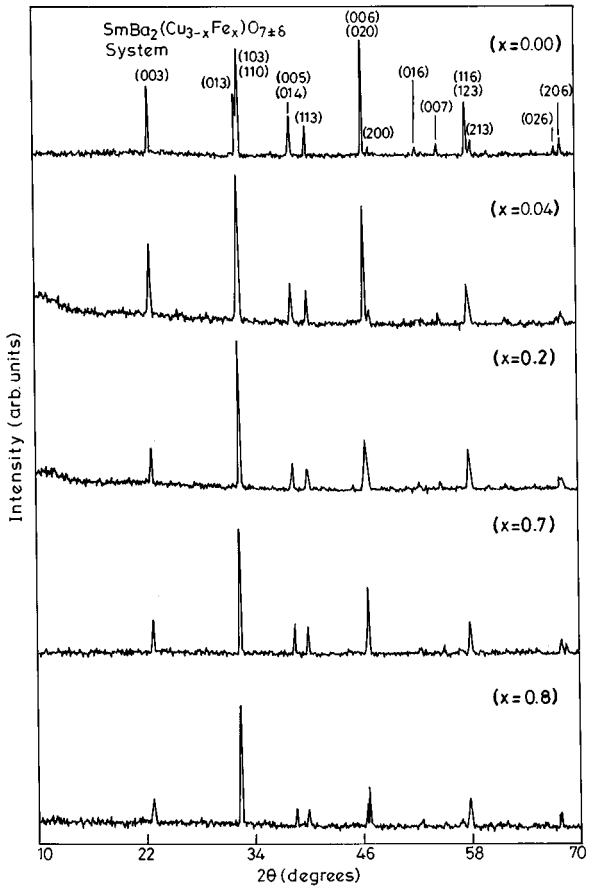

FIG. 2. XRD patterns (Cu $K\alpha$) of the $SmBa_2(Cu_{3-x}Fe_x)O_7$ system showing orthorhombic splitting for the $x=0.7$ and 0.8 compositions.

$LaBa_2Cu_{3-x}Fe_xO_7$ to be about 1.8. Thus a clear trend is observed in the solid solubility limits of the dopants with respect to the ionic size of the rare-earth ions; i.e., the solid solubility limits of 3d metal ion dopants in the 123 structure containing lighter rare earths are in general observed to be much higher than those observed for the phases containing heavier rare earths.

The lattice parameters have been calculated using the least-squares fit of the high-angle reflections (Fig. 1). The Fe-doped phases are orthorhombic at lower concentrations (x) and an O→T transition occurs at $x=0.08$. In the $SmBa_2Cu_{3-x}Fe_xO_7$ system, a second phase transition (T→O) is observed at $x=0.7$, wherein the structure changes from tetragonal to orthorhombic symmetry (Fig. 2). An O→T transition in the 123 system of compounds is generally brought about by the disordering of oxygen among the O(1) and O(5) positions. Andersen *et al.*[8] have reported that the effect of substituting Cu with Fe in Y-123 is a diminishing of the oxygen-ordered orthorhombic domain sizes and eventually a breakdown of the orthorhombic structure. Fe prefers to occupy the chain sites for lower values of x and thereby promotes a tetragonal structure. Several studies such as infrared,[9] specific heat,[10,11] Mössbauer,[10,12] x-ray absorption spectroscopy,[13] magnetic susceptibility,[14] and electron paramagnetic resonance spectroscopy of Fe-substituted Y-123 indicate the tendency for the Fe atoms to form linear clusters along the ⟨110⟩ direction with Y-123 domains separating the linear domains. The recurrence of orthorhombicity (T→O) for higher Fe content may be due to the increased clustering of the Fe ions leaving behind large Fe-free orthorhombic domains. Consequently, the size of the orthorhombic domains increases. The oxygen content determined by iodometry shows values beyond 7.0 for higher concentrations of Fe (Fig. 1).

For M=Ni, Zn, an O→T transition is observed at a higher concentration of $x=0.6$. Ni and Zn, being divalent ions, prefer to occupy the ''plane'' position [Cu(2)] and hence an O→T transition is not observed for lower values of x. At higher x, Ni occupies the Cu(1) (chain) site, also thereby bringing about an O→T transition. The c axis remains unchanged as a function of x.

The oxygen content in the $SmBa_2Cu_{3-x}Ni_xO_7$ system slightly increases to 7.07 for $x\sim0.8$ (Fig. 1). This may be attributed to the stabilization of Ni in the 3+ valence state.[15] Shimizu *et al.*[16] have reported an increase in oxygen content in the $GdBa_2Cu_{3-x}Ni_xO_7$ system due to the precipitation of NiO.

In the $SmBa_2Cu_{3-x}Zn_xO_7$ system, the oxygen content remains <7.0 for all values of x (Fig. 1). Substitution of Zn is said to promote oxygen vacancies at the O(4) site, thereby reducing the oxygen content.[7]

2. $DyBa_2(Cu_{3-x}M_x)O_7$ (M=Fe, Ni, Zn)

All compositions of the system $DyBa_2Cu_{3-x}M_xO_7$ (x =0.00–0.1 in steps of 0.02 and 0.1–0.4 in steps of 0.1) have

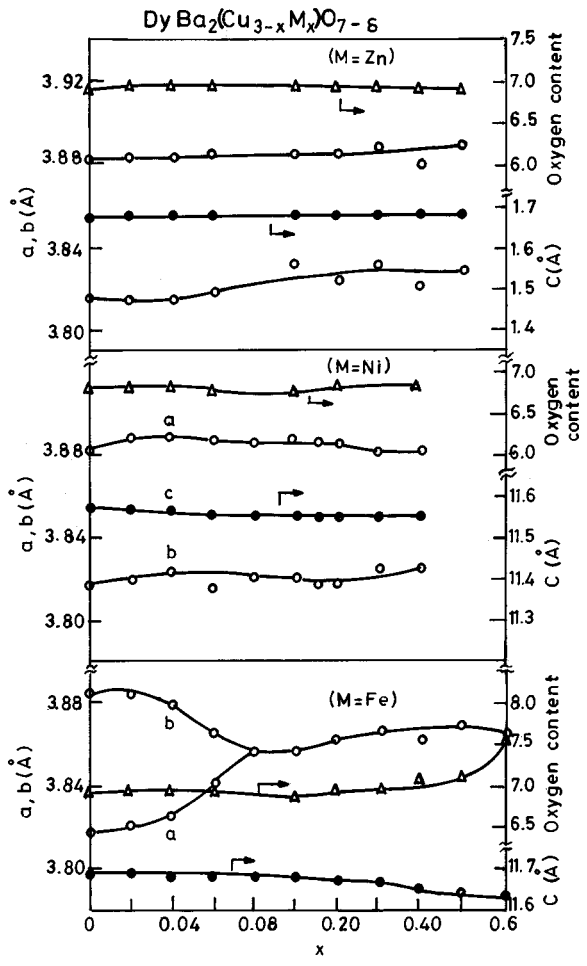

FIG. 3. Variation of lattice parameters and oxygen content as a function of concentration (x) in the $DyBa_2(Cu_{3-x}M_x)O_7$ system.

been prepared. X-ray diffraction studies indicate a maximum solid solubility of 0.6 for M=Fe, 0.4 for Ni, and 0.5 for Zn. Phases with higher concentrations of the dopants are multiphasic. The solid solubility limits are comparable to those observed in the $YBa_2Cu_{3-x}M_xO_7$ system and hence are lower than those observed in the $SmBa_2Cu_{3-x}M_xO_7$ system. The plots of lattice parameters as a function of x are shown in Fig. 3. An O→T transition is observed at x=0.1 in the $DyBa_2Cu_{3-x}Fe_xO_7$ system also. The tetragonality is retained in all the compositions 0.1–0.6 without any indication of a second phase transition (T→O). In the $DyBa_2Cu_{3-x}Ni_xO_7$ and $DyBa_2Cu_{3-x}Zn_xO_7$ systems, all the phases are orthorhombic within the limit of solid solubility.

Oxygen content values determined using iodometric titration indicate an increase in oxygen content (>7) in the Fe-doped phases as observed in the $SmBa_2Cu_{3-x}M_xO_7$ system. In the $DyBa_2Cu_{3-x}Ni_xO_7$ and $DyBa_2Cu_{3-x}Zn_xO_7$ systems, no change in the total oxygen content is observed with increasing values of x. This is similar to the observation made in the $YBa_2Cu_{3-x}Zn_xO_7$ system[5,17,18,19] where the oxygen content lies between 6.8 and 6.9.

B. Electrical, magnetic, and superconducting properties

Resistivity (ρ-T) and ac susceptibility (χ-T) studies indicate metallicity and superconductivity in the following compositions: (i) $RBa_2Cu_{3-x}Fe_xO_7$ (R=Sm, Dy; $x \leqslant 0.2$), (ii) $SmBa_2Cu_{3-x}Ni_xO_7$ ($x \leqslant 0.3$), (iii) $SmBa_2Cu_{3-x}Zn_xO_7$ ($x \leqslant 0.08$), (iv) $DyBa_2Cu_{3-x}Ni_xO_7$ ($x \leqslant 0.2$), and (v) $DyBa_2Cu_{3-x}Zn_xO_7$ ($x \leqslant 0.1$). The T_c values obtained from ρ-T and χ-T measurements are shown in Table I. The decrease in T_c is almost linear with x for lower concentrations and rapid at higher concentrations in both the systems [Figs. 4(a) and 4(b)]. The initial rates of T_c suppression (up to x=0.1) for the two systems are shown in Table II. For comparison, the corresponding values for the $YBa_2Cu_{3-x}M_xO_7$ (taken from Ref. 19) and $NdBa_2Cu_{3-x}M_xO_7$ systems (taken from Ref. 3) are also shown. As can be seen, the T_c suppression rates in the $SmBa_2Cu_{3-x}M_xO_7$ and $DyBa_2Cu_{3-x}M_xO_7$ systems lie in between those of the $NdBa_2Cu_{3-x}M_xO_7$ and $YBa_2Cu_{3-x}M_xO_7$ systems. ac susceptibility measurements have been carried out on all the superconducting phases. A few substituted phases show a granular behavior with two contributions to the diamagnetic signal (intragranular and intergranular shielding currents), characteristic of high-T_c materials.

IV. DISCUSSION

A. Mechanism of T_c suppression: AG theory

In the present system, it is appropriate to study the validity of the Abrikosov-Gor'kov (AG) pair-breaking theory in

TABLE I. The values obtained from ρ-T and χ-T measurements in $RB_2Cu_{3-x}M_xO_{7\pm x}$ (R=Sm, Dy) system.

	M=Fe				M=Ni				M=Zn			
	R=Sm		R=Dy		R=Sm		R=Dy		R=Sm		R=Dy	
Comp. x	T_c (ρ-T)	T_c (χ-T)	T_c (ρ-T)	T_c (χ-T)	T_c (ρ-T)	T_c (χ-T)	T_c (ρ-T)	T_c (χ-T)	T_c (ρ-T)	T_c (χ-T)	T_c (ρ-T)	T_c (χ-T)
0.0	90	91	90	92	90	91	90	92	90	91	90	92
0.02	84	89	88	90	83	88	83	88	81	83	81	84
0.04	78	77	82	88	83	88	82	86	70	68	70	76
0.06	71	77	78	86	76	84	81	86	59	60	62	71
0.08	68	75	74	78			77	80	49	47		
0.1	66	72	70	73	72	78	67	79	29	49	44	56
0.2	47	49	58	59	50	53	63	68			13	25
0.3		23	10	45	24	47	54	55				
0.4							31	50				

TABLE II. Solubility limits and T_c suppression rates (calculated from the initial linear slope of the T_c vs x curve) of 3d metal ions (M=Fe, Ni, and Zn) in RBa$_2$(Cu$_{3-x}M_x$)O$_7$ (R=Nd, Sm, Dy, and Y).

RBa$_2$(Cu$_{3-x}M_x$)O$_7$ (IR of R^{3+}, Å)		R=Nd (1.109) (Ref. 3)	Sm (1.079) (Present Work)	Dy (1.027) (Present Work)	Y[a] (1.019) (Present Work)
Solubility Limits	M=Fe	1.0	0.8	0.6	0.6
	Ni	0.8	0.8	0.4	0.3
	Zn	0.8	0.8	0.5	0.3
T_c suppression rates (K/at. %)	Fe	13	8	7	3
	Ni	13	7	4	3
	Zn	28	16	14	10

[a]Data taken from article by J. M. Markert, Y. Dalichaouch, and M. B. Maple, in *Physical Properties of High Temperature Superconductors*, edited by D. M. Ginsberg (World Scientific, Singapore, 1990), Vol. 1, p. 265.

view of the fact that the substituent ions are magnetic (Fe, Ni) or behave like magnetic ions (Zn). In $YBa_2Cu_3O_{7-\delta}$, the presence of magnetic rare-earth ions at the Y site produces no effect on T_c, indicating the absence of interaction of the $4f$ orbitals of the rare-earth ions with the CuO_2 planes. However, substitution at the Cu site by magnetic Fe, Ni as well as nonmagnetic Zn decreases T_c, thereby modifying the nature of interaction of the rare-earth ions with the CuO_2 planes.

According to AG theory, the reduced transition temperature is defined by the equation

$$\ln\left(\frac{1}{t}\right)=\psi\left(\frac{1}{2}+\frac{\rho}{2t}\right)-\psi\left(\frac{1}{2}\right),$$

where ψ is the digamma function, $t=T_c/T_{c0}$, and T_c and T_{c0} are the critical temperatures of the superconductor with and without impurities. ρ is the pair-breaking parameter and is given by $\rho=xN(E_F)JS(S+1)/8k_BT_{c0}$, where $N(E_F)$ is the density of states at the Fermi level and x is the concentration of magnetic impurities. If the magnetic moment is not a pure spin, but also has an angular momentum, one has to replace $S(S+1)$ by the de Gennes factor $G=(g-1)^2J(J+1)$. As expected from the AG formula, the T_c depression should follow approximately the de Gennes factor G. The T_c then decreases linearly with x for low concentrations, and at a critical concentration (x_{cr}), superconductivity completely vanishes. The T_c-vs-x plots for the $SmBa_2Cu_{3-x}M_xO_7$ and $DyBa_2Cu_{3-x}M_xO_7$ are shown in Figs. 4(a) and 4(b). The curves are AG-like. Assuming AG theory to be valid, x_{cr} has been calculated using the formula

$$x_{cr}=\frac{-\pi^2e^{-\tau}}{\dfrac{dT_c}{dx}}\left[\frac{T_{c0}}{8}\right],$$

where $\tau=-0.5772$ is the Euler's constant and T_{c0} is the T_c for $x=0$. The calculated values of x_{cr} for the Fe-, Ni-, and Zn-doped phases, respectively, are 0.25, 0.28, and 0.116 (for the Sm-123 system) and 0.31, 0.47, and 0.208 (for the Dy-123 system). Experimentally, however, we find that superconductivity is still retained for compositions with $x>x_{cr}$,

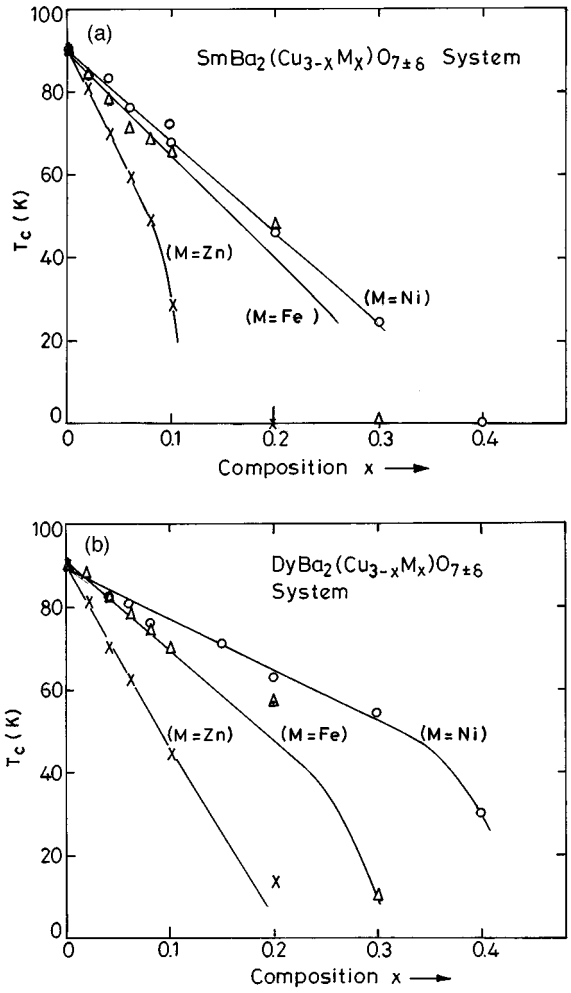

FIG. 4. (a) Variation of T_c as a function of concentration (x) in the $SmBa_2(Cu_{3-x}M_x)O_7$ system. (b) Variation of T_c as a function of concentration (x) in the $DyBa_2(Cu_{3-x}M_x)O_7$ system.

indicating a reduction in the pair breaking. This indicates that additional effects are operative in the system leading to the observed deviation from AG theory. The slight differences in the observed and calculated values may be attributed to the crystalline electric field (CEF) of the rare-earth elements. In conventional superconductors, it was shown that the pair-breaking effect of an impurity is modified due to the CEF.[20] It was found that the CEF introduces the possibility of a pair enhancement due to inelastic charge scattering involving a change in the impurity crystal-field level. The level splitting (δ) of the impurities due to the CEF leads to important modifications of AG theory. For non-Kramers ions, the ground state is nonmagnetic and the pair breaking comes from inelastic scattering and vanishes for very large energy separation of the excited states. For a Kramers ion, the ground state is always magnetic and the pair breaking results from inelastic scattering processes which are present even if the excited states have high energies. The variation of the reduced transition temperature T_c/T_{c0} as a function of impurity concentration in the presence of a non-Kramers ion and a Kramers ion is shown in Figs. 5(a) and 5(b) (taken from Ref. 20). In the latter AG-type curves are obtained for $\delta=0$ and $\delta=\infty$. Intermediate values of δ show a deviation from AG behavior.

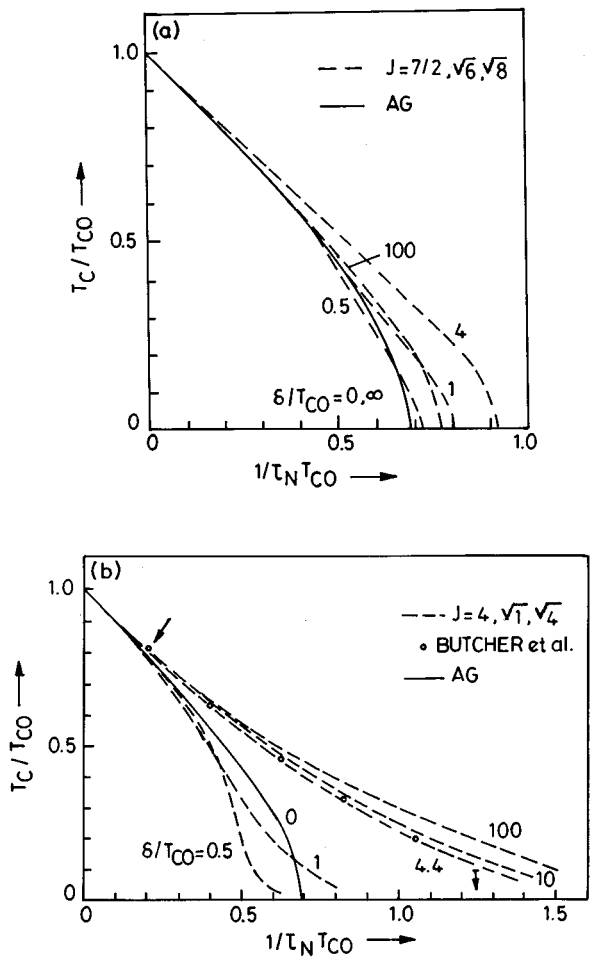

FIG. 5. T_c vs impurity concentration for alloys containing (a) Kramers ions and (b) non-Kramers ions (from Ref. 20).

In the present system, considering the fact that RBa$_2$Cu$_3$O$_{7-\delta}$ compounds are superconducting at 90 K, it appears at the outset that superconductivity is independent of the R ion. However, manifestations of CEF's such as Schottky anomalies have been observed in the low-temperature specific heat.[21] Schottky anomalies arise due to the partial lifting of the degeneracy of the ground-state multiplets of the R ions by the crystalline electric fields. Sm and Dy, being Kramers ions, it is possible that the presence of CEF's leads to a different shape of the transition temperature versus impurity concentration curve as compared to the AG behavior and can lead to lower suppression rates as a function of x, as is the case in the present study.

A comparative study of the two systems shows that the T_c suppression rates for a given M ion depend on the ionic radius of the rare earth (R), higher for the larger R ions. To explain this behavior, several possibilities need to be considered. (i) The difference in the T_c suppression rates is to a large extent due to nonmagnetic volume effects related to the lanthanide contraction. (ii) In the La-123 system, a disorder in the occupancy of La^{3+} and Ba^{2+} exists (due to ionic size compatibility) which decreases with decrease in ionic size of the rare earth from La to Y. This disorder in site occupancy is enhanced on substitution at the Cu site and is larger in the case of the Sm-123(M) system than that in the Dy-123(M) system. Consequently, the oxygen atoms in the basal plane get disordered, which weakens the coupling between the CuO chains and CuO_2 planes via the O(4) oxygen. (iii) Interaction of the rare-earth ion moments with the Cu3d-O2p orbitals leads to pair breaking. Lin *et al.*[22] have suggested a weak interaction between the Gd moments and CuO planes in the Gd-123(Ni) system based on their observation that the antiferromagnetic ordering temperature T_N decreases with increase in Ni concentration. But magnetism due to an exchange interaction alone cannot account for the T_c reduction. If this were true, then for a given dopant ion the T_c suppression rate should be larger in the DyBa$_2$Cu$_{3-x}M_x$O$_{7-\delta}$ system as compared to the SmBa$_2$Cu$_{3-x}M_x$O$_{7-\delta}$ system since the T_c reduction should scale with the de Gennes factor $G=(g-1)^2J(J+1)$. (The value of G for the Sm^{3+} ion is 4.54, whereas that of Dy^{3+} is 7.08.) On the contrary, the decrease in T_c scales with the ionic radius of the rare earth and is larger for the larger rare-earth ions. If it is possible to delineate the T_c reduction due to the nonmagnetic R ion size contribution, the magnetic pair-breaking effect could possibly be discerned. (iv) Since the T_c reduction scales with the ionic radius of the R ion, it implies that the larger spatial extension of the $4f$ orbitals of the lighter rare earths causes a hybridization of the $4f$ orbitals with the CuO_2 planes and thereby leads to localization of the mobile charge carriers in the conduction layers.

Based on the evidence available in the literature, from various substituted and unsubstituted R-123 systems, all the above mechanisms may be simultaneously operative and the situation is rather complex.

B. Mechanism of conduction in the semiconducting phases: Variable-range hopping

The semiconducting phases in the following systems are found to exhibit the phenomenon of variable-range hopping (VRH) in the temperature range 300–20 K:

(i) SmBa$_2$Cu$_{3-x}$Fe$_x$O$_7$ ($0.5 \leqslant x \leqslant 0.8$),
(ii) SmBa$_2$Cu$_{3-x}$Ni$_x$O$_7$ ($0.5 \leqslant x \leqslant 0.8$),
(iii) SmBa$_2$Cu$_{3-x}$Zn$_x$O$_7$ ($0.4 \leqslant x \leqslant 0.8$),
(iv) DyBa$_2$Cu$_{3-x}$Fe$_x$O$_7$ ($x=0.5$ and 0.6),
(vi) DyBa$_2$Cu$_{3-x}$Zn$_x$O$_7$ ($x=0.3$, 0.4 and 0.5).

The VRH mechanism of conduction is generally observed in amorphous materials whereby charge carriers are subjected to spatially randomly varying energy barriers as shown in Fig. 6(a). Anderson's theorem considers the motion of a single electron in a crystalline array of sites and on each site there is a potential well leading to a single bound s state. The energies E_j are distributed in a random way over a range V_0. If B is the band width ($B=2zI$, where z is the coordination number and I is the overlap integral, which depends on the shape of the well). Then according to Anderson's theorem, if $P=V_0/B$ is greater than some critical value P_0, then the chance that a particle placed at $t=0$ has diffused a distance r at $t=$infinity decays exponentially as $e^{-\alpha r}$, where α is the inverse localization length ($\alpha=1/a$). The absence of diffusion means that the wave functions are localized and have quantized energy. This form of localization is called Anderson localization and arises as a result of very high disorder. Under such circumstances, a finite density of states exists at E_F and all the states at E_F are localized [Fig. 6(b)].

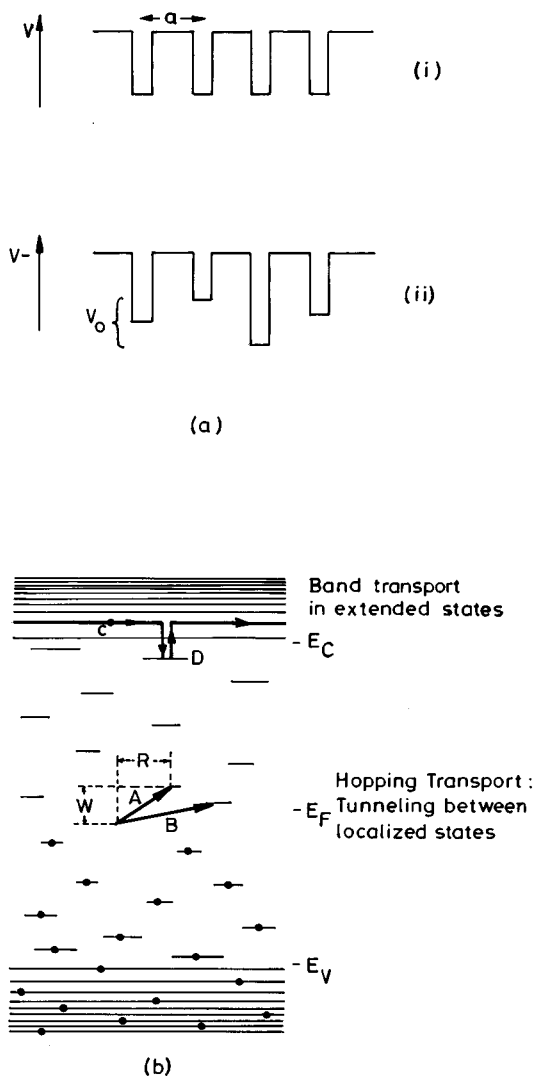

FIG. 6. (a) Potential wells for (i) a crystalline lattice and (ii) an Anderson lattice. (b) Energy level schematic for electronic conduction in an amorphous semiconductor. Energy is represented in the vertical direction and distance in the horizontal direction.

The VRH mechanism of conduction is governed by the equation $\rho=\rho_0\exp(T_0/T)^{1/d+1}$. T_0 is called the characteristic temperature and is related to the density of states at the Fermi level and the localization length as follows:

$$T_0=\beta/k_BN(E_F)a^3, \tag{1}$$

and d represents the space dimension for the hop. For two-dimensional hopping ($d=2$), $\beta=3$, and for three-dimensional hopping ($d=3$), $\beta=16$. A plot of $\ln\rho$ vs $1/T^{1/4}$ is then a straight line. Although first reported in amorphous materials, the VRH mechanism of conduction is not an uncommon phenomenon with respect to high-T_c materials. Almost all the insulating phases of high-T_c materials[23–29] exhibit the phenomenon. The temperature range over which the VRH mechanism occurs differs for different materials. E.g., in the $PrBa_2Cu_{3-x}Ga_xO_{7-\delta}$ (Ref. 31) system, three-dimensional (3D) hopping behavior is observed only in the temperature range 14–150 K and the highest value of T_0 obtained is of the order 10^9 K. It has been suggested that such a high value of T_0 is not quite reasonable and that the Mott's formula $\rho(T)=\rho_0\exp(T_0/T)^{1/4}$ is an oversimplication. In the $Y_{1-x}Pr_xBa_2Cu_3O_{7-\delta}$ (Ref. 30) system, 3D VRH behavior is observed from RT down to about 20 K. A similar 3D behavior has been observed in the $RBa_2Cu_{3-x}Ga_xO_7$ (Ref. 31) system. Fournier *et al.*[24] have reported that Fe-doped Y-123 shows hopping conduction and Fe doping greatly increases the activation energy, while Zn has a much smaller effect. Sugita *et al.*[32] have reported a 3D behavior in the $YBa_2Cu_{3-x}Fe_xO_7$ system at high temperatures and a deviation at low temperatures. They have suggested a possible crossover from 3D to 2D behavior at low temperatures. Other systems where VRH is encountered are $La_{2-x}Sr_xCuO_4$,[33,34] $La_{2-y}Sr_yCu_{1-x}Li_xO_4$,[35] $PrBa_2Cu_3O_7$,[36] $YBa_2Cu_{3-x}(Fe,Zn)_xO_7$,[37] $YBa_2Cu_3O_6$,[38] and $Bi_2Sr_2Ca_{1-x}R_xCu_2O_{8+\delta}$ (R=Nd, Sm, Gd, Dy, Y).[38,39] Non-copper-containing compounds such as $Ba_{1-x}K_xBiO_{3-y}$ and $BaPb_{1-x}Bi_xO_3$ (Ref. 40) too are known to exhibit a similar hopping behavior. Manako and Kube[41] have observed a 2D behavior in $TlBa_{1+x}La_xCuO_5$ in the temperature range between 7 and 100 K. This mechanism normally occurs only in the low-temperature region (below RT) wherein the energy is insufficient to excite the charge carriers across the Coulomb gap. Hence conduction takes place by hopping of charge carriers from one localized state to another within a small region ($\sim k_BT$) in the vicinity of E_F. In this region, the density of states remains almost a constant. Recent studies have shown that the VRH mechanism occurs over a fairly large temperature range (100–900 K).[42] This is a puzzling observation and calls for a redefinition of the VRH mechanism of charge transport.

The VRH plots ($\ln\rho$ vs $1/T^{1/4}$) for the above phases are shown in Figs. 7(a), 7(b), and 7(c) and 8(a) and 8(b). Higher concentrations of dopants show a two-slope behavior, which may be attributed to multiphonon hopping conduction.[43] The slopes progressively increase with increase in dopant concentration. The values of T_0 have been calculated from the slopes of the $\ln\rho$-vs-$1/T^{1/4}$ plots. Assuming $N(E_F)$ ($\sim 5.54\times10^{22}$) from band structure calculations,[44] the values of the localization lengths (a) have been evaluated for various compositions using Eq. (1) where $\beta=16$. The hopping range (R) and the hop energy (W) were calculated using the equations $R=[3a/2\pi N(E_F)kT]^{1/4}$ and $W=3/4\pi R^3N(E_F)$ (Tables III and IV). With increase in concentration (x), the following observations have been made in the two systems. (i) The characteristic temperature (T_0) systematically increases and the localization length (a) decreases with x indicating disorder-induced localization. The localization is therefore of the Anderson type. (ii) Higher concentrations of x show a two-slope behavior in the $\ln\rho$-vs-$1/T^{1/4}$ plot, indicating multiphonon hopping conduction. (iii) The hopping range (R) progressively decreases. This is due to the increase in disorder in the system so that conduction takes place by hopping of carriers to states located close by in space to the initial state. This normally leads to trapping of carriers and hence to the formation of small polarons. (iv) The hop energy (W) increases systematically. This implies that with increase in disorder in the system more energy is needed for the carriers to make a transition to the final state. In other words, the carriers hop to states close in space to the initial state (since R decreases), but with larger energy.

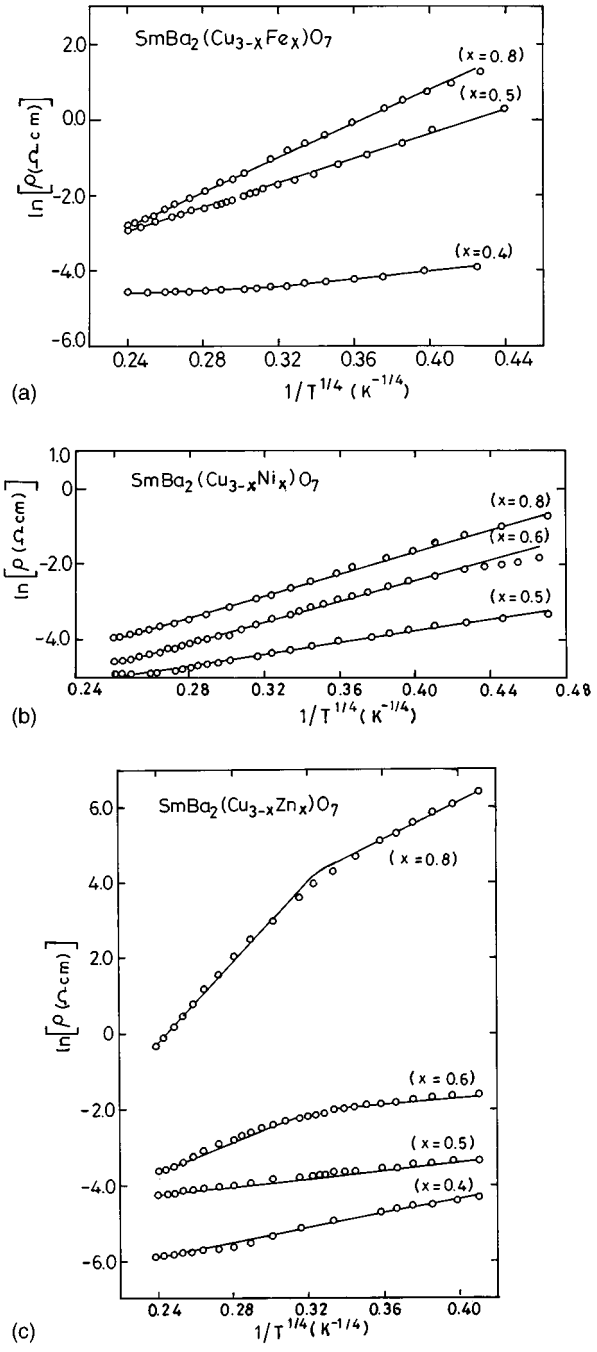

FIG. 7. Plot of ln(ρ) vs $1/T^{1/4}$ in the temperature range (T) 290–25 K, indicating the VRH mechanism in (a) $SmBa_2(Cu_{3-x}Fe_x)O_7$ ($x \geq 0.4$), (b) $SmBa_2(Cu_{3-x}Ni_x)O_7$ ($x \geq 0.5$), and (c) $SmBa_2(Cu_{3-x}Zn_x)O_7$ ($x \geq 0.4$).

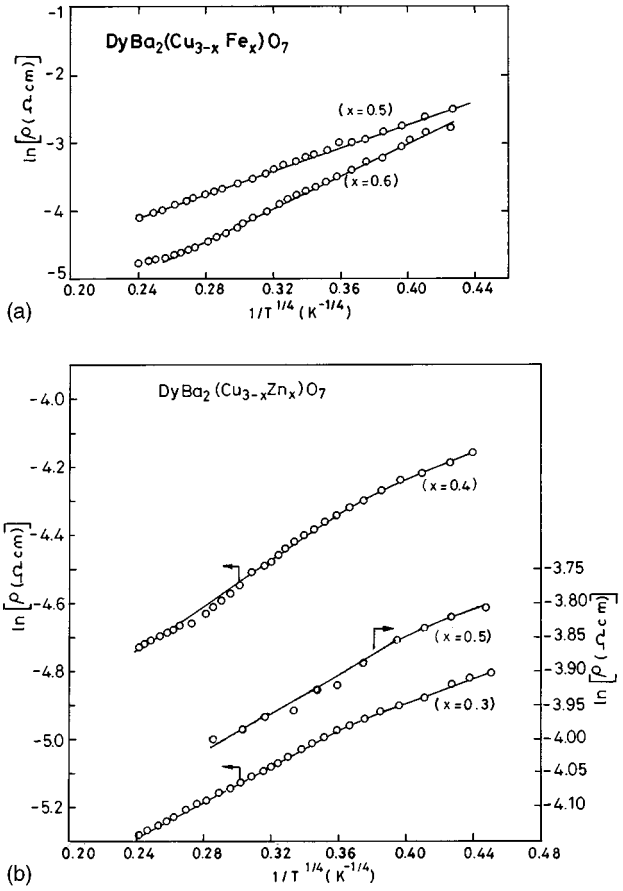

FIG. 8. Plot of ln(ρ) vs $1/T^{1/4}$ in the temperature range (T) 290–25 K, indicating the VRH mechanism in (a) $DyBa_2(Cu_{3-x}Fe_x)O_7$ ($x \geq 0.4$) and (b) $DyBa_2(Cu_{3-x}Zn_x)O_7$ ($x \geq 0.3$).

For a given concentration of the dopant as a function of temperature, it is observed that (i) T_0 and a are constants and (ii) R decreases and W increases with increase in temperature. This is as expected since at low temperatures thermal energy is less so that charge transport takes place by hopping of carriers to states with lower energy but spatially separated by large distances (R). The variation of R and W as a function of temperature is shown in Figs. 9 and 10 for the semiconducting phases of the Sm-123(M) and Dy-123(M) systems. A comparative study of the VRH mechanism in the two systems shows that (i) the T_0 values in the Sm-123(M) system (10^3–10^6 K) are higher than that of the Dy-123(M) system (10–10^5 K). (ii) It is observed that for a given dopant ion at a definite concentration (say, M=Fe and x=0.5) the values of T_0 for Sm-123(M) are larger and the localization lengths smaller than those of Dy-123(M). Since T_0 is representative of the extent of disorder in the system and is high for highly disordered materials, the present study indicates that the Sm-123(M) system is comparatively more disordered than that of the Dy-123(M) system. It also indicates that localization in the Sm-123(M) system sets in at lower x values. This is consistent with the observations made in the superconducting phases where the T_c suppression rates are higher in the Sm-123(M) system. (iii) The range (R) and hop energy (W) for a given M ion are smaller in the Sm-123(M) system than those of the Dy-123(M) system. This is a direct consequence of the larger disorder in the Sm-123(M) system, which results in shorter hopping distances as explained above. The disorder could be an electronic one arising from the interchange of the Ln^{3+} and Ba^{2+} ions.

C. Recovery of superconductivity in Zn-doped R-123 (R=Sm, Dy) by hole doping

High-temperature superconductivity (HTSC) in HTSC materials is governed by the hole concentration in the CuO_2 planes. Hence the superconducting properties can be modi-

TABLE III. Calculated parameters for the semiconducting phases in the $SmBa_2(Cu_{3-x}M_x)O_7$ system.

		Fe			Ni			Zn			
	Comp. x	0.5	0.8	0.5	0.6	0.8	0.4	0.6		0.8	
	$T_0(\times 10^3)$ K	77	204	3.6	32.2	44.9	7.7	160	39	8090	390
T(K)	a (Å)	4.2	3.0	11.6	5.6	5.0	9.0	3.3	52	0.8	24.3
20	R (Å)	13.7	12.6	17.6	14.7	14.3	16.6		25.7		21.3
	W (meV)	2.9	3.74	1.4	2.4	2.6	1.6		0.44		0.77
40	R (Å)	11.5	10.6	13.4	11.2	10.8	13.9		21.65		17.9
	W (meV)	4.9	6.3	3.1	5.3	5.9	2.8		0.74		1.30
100	R (Å)	9.2	8.5	4.6	9.8	9.6	11.1	8.62		6.06	
	W (meV)	9.7	12.4	9.8	8.0	8.5	5.6	11.6		3.36	
150	R (Å)	8.3	7.6	6.3	8.9	8.7	10.0	7.8		5.48	
	W (meV)	13.2	17	8.9	10.6	11.5	7.5	15.7		4.5	
200	R (Å)	7.7	7.1	7.6	8.3	8.1	9.30	7.25		5.09	
	W (meV)	16.3	21	8.3	13.1	14.3	9.3	19.6		5.7	
250	R (Å)	7.3	6.7	9.0	7.8	7.6	8.8	6.85		4.8	
	W (meV)	19.3	24.6	7.8	15.5	16.9	10.9	23.2		6.7	
300	R (Å)	6.96	6.4	10.6	7.5	7.3	8.4	6.55		4.6	
	W (meV)	22	28.5	7.5	17.8	19.3	12.6	26.6		7.7	

fied by either removing or adding holes depending on the material. In $YBa_2Cu_3O_7$ the hole concentration can be decreased by changing the oxygen content[45] or by doping at the Cu(1) site, which decreases the T_c and eventually destroys superconductivity at a particular concentration.

In our Zn-doped $RBa_2Cu_{3-x}Zn_xO_7$ systems, we have selected the semiconducting phases with $x=0.2$ for $R=$Sm and $x=0.3$ for $R=$Dy in order to study the effect of hole doping by Ca. Phases of the type $(Sm_{1-x}Ca_x)Ba_2Cu_{2.8}Zn_{0.2}O_7$ and $(Dy_{1-x}Ca_x)Ba_2Cu_{2.7}Zn_{0.3}O_7$ ($x=0.1$ and 0.2) have been synthesized and studied. The single-phase nature of the compounds has been established by XRD studies. Lattice parameters calculated from the high-angle reflections do not show any significant change with increasing x. Resistivity (ρ-T) and ac susceptibility (χ-T) studies indicate an increase in T_c as a function of dopant concentration (Table V). For a given

TABLE IV. Calculated parametersd of the semiconducting phases in the $DyBa_2(Cu_{3-x}M_x)O_7$ (M=Fe, Zn) system.

		Fe			Zn	
	Comp. x	0.5	0.6	0.3	0.4	0.5
T (K)	$T_0(\times 10^3)$ K	4.32	24.4	0.041	0.11	0.29
	a (Å)	10.9	6.2	51.6	37.4	24.3
20	R (Å)	17.4	15	25.7		
	W (meV)	1.4	2.2	0.44		
40	R (Å)	14.6	12.6	21.6		
	W (meV)	2.4	3.8	0.74		
60	R (Å)	13.2	11.5	19.5		
	W (meV)	3.2	4.9	1.00		
100	R (Å)	11.6	10	17.2	15.8	14
	W (meV)	4.8	7.5	1.5	1.9	2.6
150	R (Å)	10.5	9.0	15.5	14.3	12.8
	W (meV)	6.5	9.8	1.99	2.5	3.6
200	R (Å)	9.8	8.5	14.5	13.3	12
	W (meV)	7.9	12.2	2.5	3.2	4.4
250	R (Å)	9.3	8.0	13.7	12.6	11
	W (meV)	9.3	14.4	2.92	3.7	5.2
300	R (Å)	8.8	7.7	13.0	12.0	10.8
	W (meV)	10.7	16.5	3.4	4.3	5.9

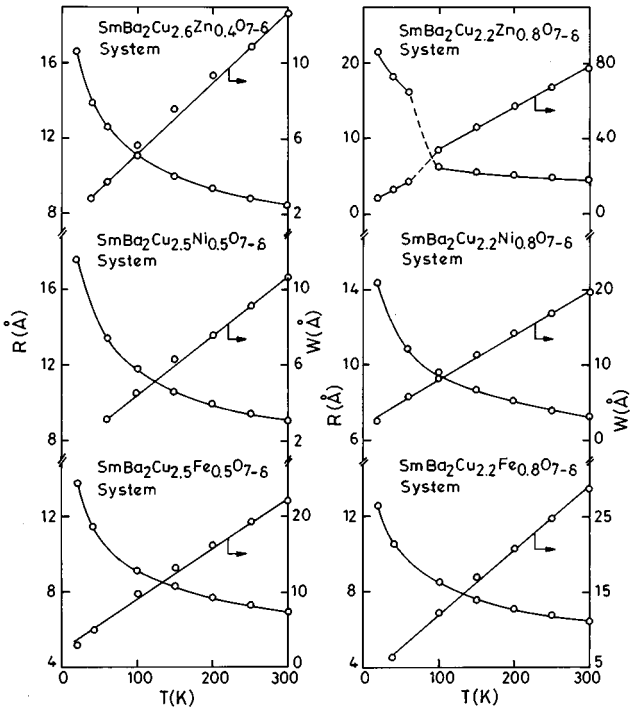

FIG. 9. Hopping range (R) and hop energy (W) as a function of temperature (T) in the SmBa$_2$(Cu$_{3-x}M_x$)O$_7$ (M=Fe, Ni, Zn) system.

x, the Zn-doped Sm-123 system shows higher T_c values compared to the Dy-123 system. In the Sm-123 system, ρ-T studies indicate a decrease in T_c from 39 K for x=0.1 to 36 K for x=0.2. T_c shifts upwards from 13 K for x=0.1 to 24 K for x=0.2 in the Zn-doped Dy-123 system. The diamagnetic onset temperatures obtained from ac susceptibility measurements are much higher than the $T_{c,0}$ values obtained from ρ-T measurements.

V. CONCLUSIONS

Systematic studies on the phase formation and electrical and magnetic properties of the RBa$_2$Cu$_{3-x}$M$_x$O$_{7\pm\delta}$ (R=Sm, Dy; M=Fe, Ni, Zn) system have indicated the following: (i) The solubility limits of M ions are higher than in the Y-123(M) system. (ii) In the Sm-123(Fe) system, a second phase transition ($T\rightarrow$O) is observed at higher concentrations similar to the Nd-123(M) system. (iii) The solubility limits and the T_c suppression rates scale with the ionic radius of the R ion; viz., the T_c suppression rates are higher in Sm-123(M) than in the Dy-123(M) system. (iv) The T_c reduction in the two systems is slower than predicted by AG. Hence the T_c suppression in R-123(M) cannot be explained in terms of magnetic exchange interactions alone. Other factors such as disorder in the site occupancy (Ln^{3+}-Ba^{2+} site exchange), crystal-field effects, etc., have to be considered. (v) A metal-insulator transition is observed at higher dopant concentrations and occurs as a result of disorder. (vi) The semiconducting phases clearly exhibit a three-dimensional (3D) variable-range-hopping (VRH) mechanism of conduction. The various parameters related to hopping; viz., the characteristic temperature T_0, the localization length (a), the range (R), and hopping energy (W) obey Anderson's localization conditions. (vii) A comparative study of two systems indicates a higher degree of disorder in the Sm-123(M) system than in the Dy-123(M) system (which arises due to interchange in site occupancy of the Ln^{3+} and Ba^{2+} ions).

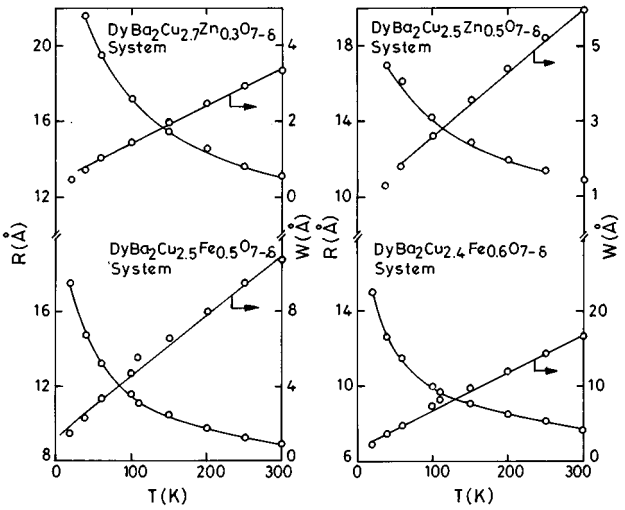

FIG. 10. Hopping range (R) and hop energy (W) as a function of temperature (T) in the DyBa$_2$(Cu$_{3-x}M_x$)O$_7$ system (M=Fe, Zn).

TABLE V. Superconductivity data on (a) the Sm$_{1-x}$Ca$_x$Ba$_2$(Cu$_{2.8}$Zn$_{0.2}$)O$_{7+\delta}$ data and (b) the Dy$_{1-x}$Ca$_x$Ba$_2$(Cu$_{2.7}$Zn$_{0.3}$)O$_{7\pm\delta}$ system.

		Resistivity data						ac susceptibility	
Comp. x	Oxygen content $7-\delta$	$T_{c,\text{onset}}$ (K)	$T_{c,0}$ (K)	ΔT_c (K)	$\rho_{300\ \text{K}}$ mΩ cm	ρ_0 mΩ cm	$d\rho/dT$ 120–300 $\mu\Omega$ cm/K	χ' T_c (K)	χ'' $T_{c,\text{peak}}$ (K)
					(a)				
0.0	6.82				2.6				
0.1	6.85	48	39	7	1.8	1.2	2.5	42	41
0.2	6.87	41	36	4	1.6	1.3	0.5	45	43
					(b)				
0.0	6.90				5.1				
0.1	6.72	19	13	5	3.3	1.0	3.0	21	18
0.2	6.78	22	30	7	2.1	2.2	4.0	28	24

This implies that the disorder decreases across the series La^{3+}–Dy^{3+}.

In conclusion, it may be stated that since the solid solubility limits and the T_c suppression rates in $RBa_2Cu_{3-x}M_xO_{7-\delta}$ scale with the ionic radii of the rare earths (R), nonmagnetic volume effects play a role in the T_0 suppression. In addition, the semiconducting phases show that the extent of disorder scales with the rare-earth ionic size. This indicates that disorder also plays a key role in the mechanism responsible for the T_c suppression.

ACKNOWLEDGMENTS

We gratefully acknowledge CEFIPRA, New Delhi for financial support. One of the authors (P.S.P.) acknowledges the NSTB-DST, New Delhi, for financial support.

[1] *Chemistry of High Temperature Superconductors*, edited by D. L. Nelson, M. S. Whittingham, and T. F. George, ACS Symp. Series No. 351 (American Chemical Society, Washington, D.C., 1987).

[2] *Novel Superconductors*, edited by S. A. Wolf and V. Z. Kresin (Plenum, New York, 1987).

[3] T. A. Mary, N. R. S. Kumar, and U.V. Varadaraju, Phys. Rev. B **48**, 16 727 (1993).

[4] Y. Xu, M. Suenaga, J. Tafto, R. L. Sebatini, A. F. Moodenbaugh, and P. Zolliker, Phys. Rev. B **39**, 6667 (1989).

[5] Y. Xu and Guan, Phys. Rev. B **45**, 3176 (1992).

[6] V. Badri and U. V. Varadaraju, Phys. Rev. B **52**, 10 504 (1995).

[7] P. R. Slater, A. J. Wright, and C. Greaves, Physica C **183**, 111 (1991).

[8] J. V. Andersen, N. H. Andersen, Ole G. Mouritsen, and H. F. Poulsen, Physica C **214**, 143 (1993).

[9] C. Jianmin, X. Leimin, Z. Yonggang, C. Peixin, and Gu Huifang, Physica C **159**, 317 (1989).

[10] B. D. Dunlop, J. D. Jorgenson, C. Segre, A. W. Dwight, J. L. Maty Kiewicz, H. Lee, W. Peng, and C. W. Kimball, Physica C **158**, 397 (1989).

[11] S. Vilminot, R. Kuentzler, Y. Dossman, A. Derory, and M. Drillon, Physica C **160**, 575 (1989).

[12] Y. Ren, W. W. Schmahl, E. Brecht, and H. Fuess, Physica C **199**, 414 (1992).

[13] C. Y. Yang, S. M. Heald, J. M. Tranquada, Y. Xu, Y. L. Yang, A. R. Moodenbaugh, D. O. Welch, and M. Suenaga, Phys. Rev. B **39**, 6681 (1989).

[14] G. Xiao, M. Z. Ceiplak, A. Garrin, F. H. Streitz, A. Baksji, and C. L. Chien, Phys. Rev. Lett. **60**, 1446 (1988); G. Xiao, M. Z. Cieplak, D. Musser, A. Gavrin, F. H. Streitz, A. Baksji, C. L. Chien, J. J. Rhyne, and J. A. Gotass, Nature **332**, 238 (1988).

[15] R. Liang, T. Nakamura, H. Kawaji, M. Itosh, and T. Nakamura, Physica C **170**, 307 (1990).

[16] H. Shimizu, T. Kiyama, and J. Arai, Physica C **196**, 329 (1992).

[17] K. Westerholt, H. W. Wuller, H. Bach, and P. Stauch, Phys. Rev. B **39**, 11 680 (1989).

[18] B. Jayaram, S. K. Agarwal, C. U. Narasimha Rao, and A. V. Narlikar, Phys. Rev. B **38**, 2903 (1988).

[19] C. S. Jee, D. Nichols, A. Kebede, S. Rahman, J. E. Crow, A. M. P. Goncalves, T. Mihalisin, G. H. Myer, I. Perez, R. E. Salomon, P. Schlottmann, S. H. Bloom, M. V. Kuric, Y. S. Yao, and R. P. Guertin, J. Supercond. **1**, 63 (1988).

[20] P. Fulde, L. L. Hirst, and A. Luther, Z. Phys. **230**, 155 (1970).

[21] M. B. Maple, J. M. Jereine, R. R. Hake, B. W. Lee, J. J. Neumeier, C. L. Seaman, K. N. Yang, and H. Zhou, J. Less Common Met. **149**, 405 (1989).

[22] C. Lin, Z. Xiao Liu, and J. Lan, Phys. Rev. B **42**, 2554 (1990).

[23] A. Podder, P. Mandal, A. N. Das, B. Ghosh, and P. Choudhary, Phys. Rev. B **44**, 2757 (1991).

[24] P. Fournier, R. Gagnon, and M. Aubin, Physica C **177**, 159 (1991).

[25] B. Fisher, G. Koren, J. Gennosa, I. Patlaggan, and E. L. Gartstein, Physica C **176**, 75 (1991).

[26] H. Taguchi, M. Nagao, and M. Shimada, J. Solid State Chem. **92**, 277 (1991).

[27] B. Jayaram, P. C. Lanchester, and M. T. Weller, Phys. Rev. B **43**, 5444 (1991).

[28] F. G. Aliev, V. Kovacik, S. R. Li, V. V. Moshchalkov, N. N. Oleinikov, N. A. Samarin, J. Sebek, and L. Sherbek, J. Magn. Magn. Mater. **90–91**, 641 (1990).

[29] Y. Xu and W. Guan, Physica C **206**, 59 (1993).

[30] Wu Jiang, P. L. Peng, J. J. Hamilton, and R. L. Greene, Phys. Rev. B **49**, 690 (1994).

[31] Y. Xu and W. Guan, Physica C **212**, 119 (1993).

[32] T. Sugita, M. Yabuuchi, K. Murase, H. Okabayashi, K. Gamo, and S. Namba, Solid State Commun. **67**, 95 (1988).

[33] B. Ellman *et al.*, Phys. Rev. B **39**, 9012 (1989).

[34] M. Z. Cieplak *et al.*, Phys. Rev. B **46**, 5536 (1992).

[35] M. A. Kastner, R. J. Birgeneau, C. Y. Chen, Y. M. Chiang, D. R. Gabbe, H. P. Jenssen, T. Junk, C. J. Peters, P. J. Picone, T. Thio, T. R. Thurston, and H. L. Tuller, Phys. Rev. B **46**, 5536 (1992).

[36] P. Fisher *et al.*, Physica C **176**, 75 (1991).

[37] P. Fournier, R. Gagnon, and M. Aubin, Physica C **177**, 159 (1991).

[38] B. Jayaram, P. C. Lancester, and M. T. Weller, Physica C **159**, P2 (1989); C. Paracchini, G. Callestani, and M. G. Francesconi, *ibid*. **167**, 249 (1990).

[39] P. Sumana Prabhu, M. S. Ramachandra Rao, U. V. Varadaraju, and G. V. Subba Rao, Phys. Rev. B **50**, 6929 (1994).

[40] C. Methfessel and S. Methfessel, in *Superconductivity in d- and f-band Metals*, edited by W. Buckel and W. Weber (Kernforschungszentrum Karlsruhe GmbH, Karlsruhe, 1982), p. 393.

[41] T. Manako and Y. Kubo, Phys. Rev. B **50**, 6402 (1994).

[42] V. Ponnambalam and U. V. Varadaraju, Phys. Rev. B **52**, 16 213 (1995).

[43] M. L. Knotek and M. Pollak, Phys. Rev. B **9**, 664 (1974); D. Emin, Phys. Rev. Lett. **32**, 303 (1974).

[44] W. E. Pickett, R. E. Cohen, and H. Krakauer, Phys. Rev. B **42**, 8764 (1990).

[45] R. J. Cava, A. W. Hewat, E. A. Hewat, B. Batlogg, M. Marezio, K. M. Rabe, J. J. Krajewski, W. F. Peck, Jr., and L. W. Rupp, Jr., Physica C **165**, 419 (1990).